
zip2zip: Inference-Time Adaptive Tokenization via Online Compression

Saibo Geng^{1*} Nathan Ranchin^{1*} Yunzhen Yao¹ Maxime Peyrard⁴

Chris Wendler^{1,2} Michael Gastpar¹ Robert West¹

¹EPFL ²Northeastern University

⁴Université Grenoble Alpes, CNRS, Grenoble INP, LIG

{saibo.geng, nathan.ranchin, yunzhen.yao, michael.gastpar, robert.west}@epfl.ch
maxime.peyrard@univ-grenoble-alpes.fr ch.wendler@northeastern.edu

Abstract

Tokenization efficiency plays a critical role in the performance and cost of large language models (LLMs), yet most models rely on static tokenizers optimized on general-purpose corpora. These tokenizers’ fixed vocabularies often fail to adapt to domain- or language-specific inputs, leading to longer token sequences and higher computational costs. We introduce zip2zip, a novel method for achieving context-adaptive tokenization in LLMs at inference time. Leveraging an online data compression algorithm (Lempel–Ziv–Welch), zip2zip dynamically expands its active vocabulary at inference time by continuously replacing fragmented token sequences with more compact hypertokens, which it can immediately output during generation. zip2zip consists of three key components: (1) a tokenizer based on Lempel–Ziv–Welch compression that incrementally merges co-occurring tokens into reusable hypertokens on the fly; (2) a dynamic embedding (and unembedding) layer that computes embeddings for newly formed hypertokens at runtime; and (3) a variant of autoregressive language modeling that pretrains the model to handle hypertokenized, compressed text sequences as inputs and outputs. We show that an existing LLM can be uptrained for zip2zip in 10 GPU-hours via parameter-efficient finetuning. The resulting LLM performs test-time adaptation, learning to use hypertokens in unseen contexts and reducing input and output tokens by 15–40%. Code and models are released at <https://github.com/epfl-dlab/zip2zip>.

1 Introduction

Large language models (LLMs) have shown impressive versatility across a broad spectrum of tasks and domains [Brown et al., 2020, Bubeck et al., 2023], including biomedical tests [Nori et al., 2023], mathematical reasoning [Frieder et al., 2023], programming [Jiang et al., 2024], and multiple human languages. A critical underlying component of this flexibility is the tokenizer, which defines the model’s vocabulary and governs how raw text is converted into token sequences fed to the model. The efficiency of the tokenization scheme—i.e., how compactly a text is represented as tokens—has significant impact on model performance. In particular, a more compact tokenization yields three key benefits: (1) larger effective context windows; (2) lower computational (and thus monetary) cost; and (3) shorter response times.

Despite its importance, the tokenizers used in most LLMs operate with fixed, static vocabularies obtained by running algorithms such as Byte Pair Encoding [Sennrich et al., 2016] over large-scale, general-purpose web corpora. While this globally optimized vocabulary performs reasonably well on average, it often fails to adapt to domain-specific or language-specific distributions [Ahia et al., 2023,

*Equal contribution.

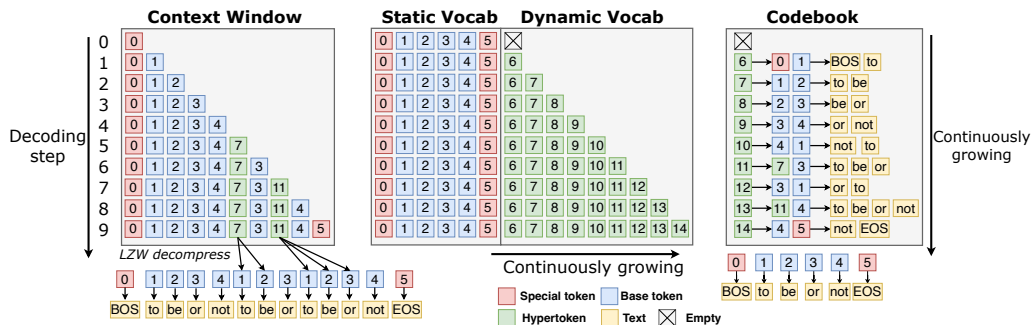


Figure 1: **zip2zip inference process.** At each decoding step, the model has a growing **context** composed of both **base tokens** (blue) and **hypertokens** (green). The **static vocabulary** of size 6 remains fixed, while the **dynamic vocabulary** is continuously expanded by merging co-occurring tokens using **LZW compression**. The **codebook** (right) maps hypertoken IDs to their corresponding base tokens. As decoding progresses, new hypertokens created at step t (e.g., “to be”, “or not”) become immediately available for reuse at step $t + 1$. Hypertokens are also eligible for merging, enabling the formation of **nested hypertokens**. The final output sequence (bottom) is reconstructed via LZW decompression.

Petrov et al., 2023], where the text distribution diverges significantly from the pretraining data. The resulting mismatch leads to longer token sequences, increasing both memory and compute demands, as well as the end user’s cost by a factor of 2–3x when processing domain-specific text [Ahia et al., 2023]. To mitigate this issue, prior work has explored expanding the token vocabulary during domain or language adaptation to improve tokenization efficiency [Wang et al., 2019, Zhao et al., 2024, Kim et al., 2024, Liu et al., 2023, 2024a]. While effective, this approach needs to be repeated for each target domain or language and requires maintaining separate tokenizers. Meanwhile, commercial LLM providers trend toward increasing the size of token vocabularies—growing from 32K to 128K [Grattafiori et al., 2024] and even up to 200K [Abdin et al., 2024] tokens—to improve overall tokenization efficiency. However, prior work [Dagan et al., 2024, Liang et al., 2023] shows that simply enlarging the vocabulary yields diminishing returns in domain adaptation, and vocabularies past a certain size can potentially degrade model performance [Liang et al., 2023]. These limitations point to a compelling need for an adaptive tokenization mechanism—one that can dynamically tailor the vocabulary to the input text at inference time, without retraining the model or maintaining separate tokenizers. Such a mechanism would allow the model to construct new domain-specific tokens on-the-fly, so as to enhance tokenization efficiency. However, adaptive tokenization poses architectural challenges, as both the embedding layer and the language modeling head in transformer models [Vaswani et al., 2017] are static matrices tied to a fixed vocabulary size.

In this paper, we propose zip2zip (with a hat-tip to seq2seq [Sutskever et al., 2014]), a novel building block that brings inference-time adaptive tokenization to LLMs. zip2zip comprises three key components: (1) **LZW tokenizer:** A tokenizer that integrates the Lempel–Ziv–Welch² compression algorithm on top of Byte Pair Encoding (BPE) [Welch, 1984]. By applying the LZW compression algorithm to the base token sequence—continuously merging frequently co-occurring token sequences into reusable longer tokens (hypertokens)—the resulting tokenization becomes less fragmented and more compact. (2) **Dynamic-embedding architecture:** An augmentation of the transformer architecture with a lightweight encoder that replaces the static embedding matrix, allowing the model to compute embeddings for newly formed hypertokens on the fly. (3) **Pretraining under online token compression:** a variant of causal language modeling that trains the model directly on LZW-compressed sequences, aligning learning with the inference-time (hyper)token distribution. The overall process is illustrated in Figure 1, which shows how the context window, dynamic vocabulary, and codebook evolve together during decoding. The name zip2zip reflects its dual role in achieving compression of both the input tokens (the first *zip*) and output tokens (the second *zip*), thereby jointly improving the efficiency of input encoding and output decoding. We conduct continued pretraining on Phi-3-4B and Phi-3.5-14B to support zip2zip using as few as 100M tokens. The resulting models demonstrate strong inference-time compression capabilities across various domains, achieving 15–40% reductions in sequence length and up to 40% improvements in end-to-end latency.

²LZW is the algorithm used in the ZIP compression tool, which inspired the name zip2zip.

To make it easy to upgrade existing LLMs to zip2zip, we release an efficient, open-source implementation of the training and inference stack. It includes (1) a fast Rust-based LZW tokenizer, (2) a drop-in model architecture compatible with HuggingFace Transformers, (3) a training pipeline for LZW-compression-based finetuning. Existing LLMs can be seamlessly extended with zip2zip, gaining adaptive tokenization capabilities through parameter-efficient finetuning.

2 zip2zip

2.1 Dynamic Token Vocabulary

To enable dynamic tokenization at inference time, we associate the LLM with a *hyper-vocabulary* \mathcal{V}_h that augments the model’s static token vocabulary. Tokens from the original vocabulary \mathcal{V} are referred to as *base tokens*. Each entry in the hyper-vocabulary is a *hypertoken*, representing a merged sequence of base tokens. The total vocabulary for a zip2zip model is the union $\mathcal{V} \cup \mathcal{V}_h$. At the beginning of each inference session, \mathcal{V}_h is initialized as an empty set, and is incrementally populated during decoding by identifying and merging recurring token subsequences in the context window, as illustrated in Figure 1.

Continuous Vocabulary Expansion. As decoding proceeds, zip2zip continuously merges co-occurring tokens into new hypertokens and recursively applies merging on new hypertokens. This *continual expansion* allows the model to represent longer, recurring sequences of base tokens compactly. Hypertokens are treated as first-class tokens within the model, used interchangeably with base tokens throughout the decoding process. Importantly, this process occurs entirely during inference, without modifying the underlying tokenizer or requiring model retraining.

LZW Algorithm. We implement vocabulary expansion using the Lempel–Ziv–Welch (LZW) compression algorithm—a dictionary-based, lossless compression method that incrementally builds a codebook of variable-length sequences. In our setting, the codebook is initialized with the base token vocabulary \mathcal{V} and expands by adding new hypertokens on the fly as recurring token patterns are encountered. To control the growth of the dynamically expanding vocabulary, we impose a maximum merge size M that restricts how many base tokens a single hypertoken can represent. LZW is particularly well-suited for zip2zip due to the following properties:

- (1) it is **online**: hypertokens created at step t can be immediately reusable at step $t + 1$; in contrast, methods like BPE require access to the full sequence and operate offline;
- (2) it is **self-contained**: input base tokens can be perfectly reconstructed from the compressed token sequence alone;³
- (3) it is **unambiguous**: when both base tokens and hypertokens are available, which one to use is consistently determined by the LZW algorithm without ambiguity.

2.2 Hyper-Embedding and Hyper-Unembedding

Hypertokens do not have fixed embedding vectors in the original model’s embedding layer (and unembedding layer), as they are not part of the original vocabulary. To compute the embedding of a hypertoken, we learn a mapping from the base token embeddings to the hypertoken embedding. We achieve this by introducing a *hyper-encoder*, which is a neural network that takes the embeddings of the constituent base tokens as input and outputs the corresponding hypertoken embedding (see Figure 2(a)). Specifically, for a sequence of M base tokens $y_{1:M} := y_1 \dots y_M$, the hyper-encoder $f_\phi : \mathcal{V}^M \rightarrow \mathbb{R}^d$ produces the hypertoken embedding $h = f_\phi(y_{1:M}) \in \mathbb{R}^d$, where M is the maximum merge size and d is the embedding dimension. For hypertokens composed of fewer than M base tokens, we pad the input sequence to length M . Since the embedding map for base tokens remains unchanged, the hyper-encoder f_ϕ essentially maps the concatenated base token embeddings from an $(M \times d)$ -dimensional space to a d -dimensional hypertoken embedding vector, performing nonlinear dimensionality reduction. For the output unembedding layer, if the underlying transformer ties the embedding and the unembedding matrices, one can reuse the same hyper-encoder to compute the representation used for unembedding. Otherwise, a separate hyper-encoder is trained to produce the hypertoken unembedding vectors.

³There is no need to persist or transmit the codebook across inference calls, preserving compatibility with existing LLM libraries and interfaces.

consistently can result in two types of errors: (1) hypertokens that cannot be decoded, or (2) the model attempting to decode a non-existing hypertoken.

Hyper-Embedding Cache. Although hypertoken embeddings are computed on-the-fly, they are context-independent and can thus be cached across inference steps. Similar to the transformer’s KV-cache, this enables *incremental* updates: only newly created hypertokens need to be embedded at each step. Since the codebook grows linearly with the number of tokens in the context, the total cache size also grows linearly in memory. Thus, the computational cost for hypertoken embeddings remains constant per step—i.e., one token embedding is computed per step.

2.4 zip2zip Pretraining

Objective. Let \mathcal{D} denote the target text distribution. Given a language model π_θ parameterized by θ , standard pretraining seeks to minimize the causal language modeling (CLM) objective (see Figure 2(b)), which corresponds to the expected negative log-probability of data sequences under the model:

$$\min_{\theta} \mathbb{E}_{y \sim \mathcal{D}} [-\log \pi_\theta(y)], \quad (1)$$

where $\pi_\theta(y)$ denotes the probability of the token sequence y under the model π_θ .

Let \mathcal{C} be an *online* compression algorithm (e.g., LZW), and ϕ be the parameters of the hyper-encoder. Given a sequence $y \sim \mathcal{D}$, let $z = \mathcal{C}(y)$ be its compressed form. In zip2zip, we aim to optimize the same CLM loss, but over the compressed sequences z . The training objective becomes:

$$\min_{\theta, \phi} \mathbb{E}_{y \sim \mathcal{D}} [-\log \pi_{\theta, \phi}(\mathcal{C}(y))] = \min_{\theta, \phi} \mathbb{E}_{z \sim \mathcal{C}(\mathcal{D})} [-\log \pi_{\theta, \phi}(z)]. \quad (2)$$

Here, we slightly abuse the notation to let $\pi_{\theta, \phi}(z)$ denote the probability assigned to the compressed sequence z , parameterized by the base model weights θ and the hyper-encoder parameters ϕ .

To construct the compressed dataset $\mathcal{C}(\mathcal{D})$, we first tokenize the corpus using a standard tokenizer, and then apply the LZW compression algorithm. This preprocessing step is performed once prior to training and can be efficiently parallelized through batching. Compression is applied at the document level, meaning that each document is compressed independently. This prevents the compressor from learning patterns across unrelated documents.

Parallelizable Training via Causal Masking. Although hypertokens introduce additional vocabulary dynamics, training remains fully parallelizable. We leverage the standard causal masking mechanism used in language models, allowing the model to predict the next token—whether a base token or a hypertoken—at each position in parallel. To eliminate the need for sequential codebook updates during inference, we precompute a fixed codebook by applying LZW compression to the entire input sequence. This precomputed codebook is then used consistently throughout training to condition token predictions, ensuring efficiency and compatibility with standard training pipelines.

Auxiliary Reconstruction Loss. We introduce an auxiliary reconstruction objective that encourages a hypertoken embedding to retain sufficient information about its underlying base token sequence (see Figure 2(c)). Specifically, the model is trained to reconstruct the original base token embeddings from the hypertoken embedding. We jointly optimize the language model and the hyper-encoder using a combined loss that includes both the standard next-token prediction loss and the auxiliary reconstruction loss. Formally, we optimize:

$$\min_{\theta, \phi, \psi} \mathbb{E}_{y \sim \mathcal{D}} [-\log \pi_{\theta, \phi}(\mathcal{C}(y))] + \lambda \mathbb{E}_{y_{1:M}} [\Delta(y_{1:M}, f_\psi(f_\phi(y_{1:M})))], \quad (3)$$

where $f_\phi : \mathcal{V}^M \rightarrow \mathbb{R}^d$ is the hyper-encoder, $f_\psi : \mathbb{R}^d \rightarrow \mathcal{V}^M$ is the decoder aiming to reconstruct the corresponding base tokens from their hyper-embedding, and $\Delta : \mathcal{V}^M \times \mathcal{V}^M \rightarrow \mathbb{R}$ is the reconstruction loss function, such as the cross-entropy loss, between the base tokens $y_{1:M}$ and the reconstructed base tokens $f_\psi(f_\phi(y_{1:M}))$. The hyperparameter $\lambda \geq 0$ controls the trade-off between the prediction error of the language model and the reconstruction error of the autoencoder. This joint optimization objective encourages the hyper-encoder to learn a compact d -dimensional manifold embedded in the higher-dimensional $(M \times d)$ space of base token embeddings, while the language model $\pi_{\theta, \phi}$ learns to predict the next (hyper)token given the preceding context. The reconstruction loss can be viewed as a form of auto-encoding, where the hypertoken acts as a compressed latent representation and reconstruction encourages the preservation of semantic content and the compression to be lossless.

Adapting Pretrained Language Models. Retraining large language models from scratch is computationally expensive and often infeasible for most research labs. A more economical alternative is to perform continued pretraining (or adaptation) on existing pretrained model weights. The proposed objectives (Equations 2, 3) integrate naturally into this setup. Parameter-efficient methods such as LoRA [Hu et al., 2022] may also be used, which allow selectively updating parts of the base model weights with minimal computational cost.

2.5 Efficiency Advantage

zip2zip improves efficiency by increasing the average token length, thereby reducing the number of tokens required to represent the same text. This compression applies to both inputs (e.g., prompts) and outputs (e.g., completions). As a result, the model performs fewer computations—both in the attention mechanism and the feedforward layers—and, more importantly, requires fewer autoregressive decoding steps during inference. Since the latency of large language models is primarily driven by the cost of sequential decoding, reducing the number of output tokens by $n\%$ leads to an approximate $n\%$ speedup in decoding latency, which we will demonstrate empirically in Section 3.6. A more detailed discussion of FLOPs is provided in Appendix E for completeness.

2.6 Entropy Invariance under Lossless Compression

Before turning to empirical results, we analyze whether a lossless compression of the data representation can fundamentally alter the achievable performance of a model. We show that for any lossless mapping g , there always exists a corresponding *transported model* distribution in the compressed space that achieves exactly the same (cross-)entropy as in the original space.

Let \mathcal{X} be the original alphabet and \mathcal{Z} an arbitrary alphabet obtained via a lossless compressor $g: \mathcal{X}^* \rightarrow \mathcal{Z}^*$, which is a bijection onto its image. Denote by P_X the true distribution over sequences $x \in \mathcal{X}^*$, and by p_θ the model distribution on the same space. The corresponding push-forward (compressed-space) true distribution P_Z and model distribution p_γ are defined as

$$P_Z(z) = P_X(g^{-1}(z)), \quad p_\gamma(z) = p_\theta(g^{-1}(z)), \quad z \in \mathcal{Z}^*.$$

Theorem 2.1 (Entropy invariance under lossless compression). *If g is lossless (i.e., bijective onto its image), then the total entropy and cross-entropy are invariant under the transformation:*

$$H(P_Z) = H(P_X), \quad H(P_Z, p_\gamma) = H(P_X, p_\theta).$$

A detailed proof is provided in Appendix G.

The theorem implies that the optimal achievable cross-entropy in the compressed representation is identical to that in the original domain: for any model family on \mathcal{X}^* , one can always construct a corresponding model family on \mathcal{Z}^* via push-forward that attains the same likelihood. In practice, the training process can be viewed as an attempt to approximate this *transported model* through optimization; however, convergence to the target model is not guaranteed (see Section 5).

3 Experiments

To evaluate the effectiveness of zip2zip, we perform continued pretraining on the Phi-3 models (3B and 14B) within the zip2zip framework. We train a single model on a general-purpose corpus and evaluate it across four dimensions: (1) token efficiency, (2) language modeling perplexity, (3) downstream task performance, and (4) inference efficiency. This setup allows us to assess how well zip2zip generalizes to diverse domains without any task- or domain-specific fine-tuning. For perplexity and downstream benchmarks, we use the widely adopted *lm-evaluation-harness* framework [Gao et al., 2024].

3.1 Training Setup

Rather than updating the full model weights, we adopt parameter-efficient finetuning using LoRA [Hu et al., 2022]. In addition, we train the *hyper-embedding* and *hyper-unembedding* modules. We set the maximum merge size to $M = 3$ and use a two-layer transformer encoder as the hyper-encoder.

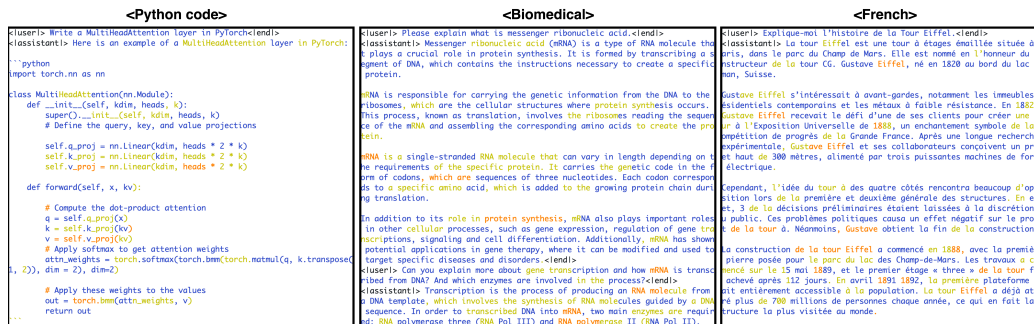


Figure 4: **Phi-3.5-zip2zip output examples.** **Blue:** base tokens. **Yellow:** hypertokens (composed of 2 base tokens). **Orange:** hypertokens (composed of 3+ base tokens).

Table 1: Examples of hypertokens formed by Phi-3.5-zip2zip across three domains

Code Generation	Biomedical	French
tor + ch = torch	m + R + NA = mRNA	E + iff + el = Eiffel
Att + ention = Attention	trans + cribed = transcribed	de + la = de la
Multi + Head = MultiHead	synth + esis = synthesis	Gust + ave = Gustave
k + dim = kdim	cell + ular = cellular	comm + enc + é = commencé

The loss weighting coefficient λ was chosen to be 0.1, as justified in Appendix I. Ablation studies on M and the hyper-encoder architecture can be found in Appendix C. For comparison, we also perform continual pretraining of the base model using LoRA under identical training conditions, serving as a baseline (denoted as Cont. Pretraining in the tables). The continual pretraining process is highly efficient, requiring approximately 10 H100-GPU hours for a 4B-parameter model and up to 40 H100-GPU hours for a 14B-parameter model, using only 0.1 billion training tokens. Interestingly, the *reconstruction loss* converges to near zero during continued pretraining, indicating that the model can almost perfectly recover the original base token sequences from the hypertoken representations. This highlights the learned compression is highly information-preserving. Details of the training setup, compute infrastructure, and dataset curation are provided in Appendices I and J.

3.2 Qualitative Examples and Hypertoken Patterns

We present several examples (Figure 4 and Table 1) to provide intuition into how the zip2zip model generates text. We see that the model generates a mixture of hypertokens and base tokens in the output (Figure 4). The hypertoken ratio is as high as 40% in the Python code generation example, and 20% in the biomedical text generation example. Many of the hypertokens correspond to semantically meaningful units or domain-specific terms as shown in Table 1. For a more fine-grained visualization of hypertoken with zip2zip, we provide visualizations of token streams in Figure 10 in the appendix.

3.3 Token Efficiency

Given an input text x and a tokenizer, we define the *token efficiency* $\eta := \frac{\text{Bytes}(x)}{\text{Tokens}(x)}$ as the average number of bytes represented by each token (also called *compression ratio*), where $\text{Bytes}(x)$ refers to the number of bytes in the UTF-8 encoding of x . This measures how compactly a tokenizer encodes input text—higher values of η indicate more efficient tokenization. We evaluate token efficiency using the tokenizers of four LLMs—Llama-3 [Grattafiori et al., 2024], Qwen-2 [Yang et al., 2024], Phi-4 [Abdin et al., 2024], and Gemma-3 [Team, 2025]—each associated with a different base vocabulary size ranging from 128K to 256K. Token efficiency is measured across five representative domains, sampled from publicly available datasets: code [Lozhkov et al., 2024b], math [LI et al., 2024], chat [Ding et al., 2023], multilingual [Penedo et al., 2024], and web [Lozhkov et al., 2024a]. Table 2 shows that applying LZW zip2zip consistently improves token efficiency across all tokenizer and domains. Gains are particularly strong in structured domains like code and math—with gains of 48% and more over the base tokenizer. Interestingly, models with larger vocabulary sizes do not always achieve better token efficiency, suggesting that simply enlarging the vocabulary size is not sufficient to improve it.

Table 2: Token efficiency (bytes per token) across domains for different tokenizers with and without zip2zip.

Tokenizer	Code	Math	Chat	Multilingual	Web
Llama-3-128K [Grattafiori et al., 2024]	4.1	2.7	5.1	3.8	4.6
+zip2zip	6.3 (+54%)	4.0 (+48%)	6.4 (+25%)	4.7 (+24%)	5.4 (+17%)
Qwen-2-150K [Yang et al., 2024]	4.0	2.3	5.1	3.7	4.4
+zip2zip	6.2 (+55%)	3.7 (+61%)	6.4 (+25%)	4.6 (+24%)	5.2 (+18%)
Phi-4-200K [Abdin et al., 2024]	4.1	2.7	5.4	4.6	4.7
+zip2zip	6.3 (+54%)	4.1 (+52%)	6.7 (+24%)	5.5 (+20%)	5.4 (+15%)
Gemma-3-256K [Team, 2025]	3.3	2.3	5.0	4.4	4.5
+zip2zip	5.6 (+70%)	3.7 (+61%)	6.4 (+28%)	5.4 (+23%)	5.4 (+20%)

3.4 Perplexity

We evaluate the perplexity of zip2zip models on four corpora: Wikitext [Merity et al., 2016], The Pile [Gao et al., 2020], and two subsets of Paloma [Magnusson et al., 2023]: mC4, a multilingual subset of C4, and dC4 (aka C4-100D), a subset of C4 spanning 100 domains. Given a token sequence $x = x_1, \dots, x_N$, and a model q , perplexity and byte-level perplexity [Radford et al., 2019, Magnusson et al., 2023] are defined as: $\text{PPL} := \left(\prod_{i=1}^N q(x_i)\right)^{-1/N}$, $\text{Byte-PPL} := \left(\prod_{i=1}^N q(x_i)\right)^{-1/B} = \text{PPL}^{1/\eta}$, where B is the number of UTF-8 bytes of the text, and η denotes the token efficiency (i.e., bytes per token). Token-level perplexity depends on the tokenization scheme and is unsuitable for cross-tokenizer comparison. We instead report byte-level perplexity, a vocabulary-agnostic metric that normalizes for tokenization differences. Table 3 (right panel) shows that zip2zip models see a modest increase in byte-level perplexity, indicating a slight drop in language modeling performance.

Table 3: Two-shot accuracy across seven NLP benchmarks (left) and byte-level perplexity (\downarrow) on four corpora using a 1024-token context window (right). Standard deviations (bootstrapped) ≈ 0.02 across all tasks.

Model	Method	ARC-c	ARC-e	HS	OBQA	PIQA	WG	GSM8K	Wiki	Pile	mC4	dC4
Phi-3.5-4B	Base	0.60	0.83	0.66	0.46	0.79	0.75	0.82	1.58	1.79	1.88	1.74
	Cont. pretrain	0.60	0.82	0.63	0.47	0.82	0.75	0.40	1.59	1.81	1.88	1.74
	zip2zip	0.57	0.83	0.61	0.46	0.82	0.75	0.15	1.69	1.95	2.00	1.82
Phi-3-14B	Base	0.62	0.80	0.70	0.51	0.83	0.76	0.84	1.43	1.72	1.82	1.67
	Cont. pretrain	0.62	0.88	0.66	0.52	0.87	0.80	0.52	1.47	1.79	1.86	1.68
	zip2zip	0.62	0.86	0.68	0.51	0.85	0.79	0.25	1.56	1.90	1.96	1.75

3.5 Evaluation on NLP Benchmarks

We next evaluate zip2zip’s few-shot performance on real-world tasks. We evaluate on seven widely used NLP benchmarks, including ARC-[Challenge, Easy] [Clark et al., 2018], HellaSwag [Zellers et al., 2019], LAMBADA [Paperno et al., 2016], OpenbookQA [Mihaylov et al., 2018], PIQA [Bisk et al., 2019], Winogrande [Sakaguchi et al., 2019] and GSM8K [Cobbe et al., 2021]. As shown in Table 3, the model continued-pretrained with zip2zip performs similarly to the baseline on most tasks. However, on GSM8K, where the primary task involves numerical computation, the model exhibits significant degradation. While token-level operations are already known to be challenging for LLMs [Singh and Strouse, 2024], it is possible that adaptive tokenization exacerbates this effect, though further validation is required to confirm this hypothesis.

Multilinguality. To validate the effectiveness of zip2zip on non-English languages, we evaluate the model on machine translation tasks, including WMT14 [Macháček and Bojar, 2014], WMT16 [Bojar et al., 2016]. The results, shown in Table 4, indicate a small performance degradation across the BLEU, CHRF, and TER metrics when using zip2zip. However, the drop is relatively minor, suggesting that the model retains strong multilingual capabilities even in the compressed representation. Additional experiments on multilingual QA benchmarks are provided in Appendix H.2.

Table 4: Machine translation performance on WMT benchmarks. Scores are averaged across both translation directions. Standard deviations (approximately 1.0 ~ 2.0) are reported in Table 11 in Appendix H.

Model	Method	WMT14 En-Fr			WMT16 En-De			WMT16 En-Ro		
		BLEU↑	CHRf↑	TER↓	BLEU↑	CHRf↑	TER↓	BLEU↑	CHRf↑	TER↓
Phi-3.5-4B	Base	33.6	58.3	53.0	39.2	63.2	47.9	17.7	45.5	73.4
	Cont. pretrain	36.5	61.0	51.5	42.3	65.4	44.9	16.7	45.8	79.7
	zip2zip	34.1	59.4	54.5	39.7	64.5	48.0	14.3	44.2	93.5
Phi-3-14B	Base	39.1	62.6	49.3	43.1	65.6	44.1	21.3	51.0	70.5
	Cont. pretrain	38.9	63.2	48.8	48.4	70.1	39.8	21.8	52.0	68.3
	zip2zip	36.4	62.8	51.2	44.8	68.1	42.9	19.5	50.1	72.9

3.6 Inference Efficiency

zip2zip reduces decoding time by lowering the number of tokens that need to be generated. However, it introduces additional FLOPs due to the on-the-fly computation of hyper-embeddings by the hyper-encoder. To address this overhead, we implement hyper-embedding caching and optimize the computation using a custom Triton kernel. We report separate timings for *prefilling* and *decoding* across multiple models, with and without zip2zip, in Table 5. As we show in Table 5, zip2zip achieves a significant speedup in all four settings. Both prefilling and decoding times are significantly reduced, with the most substantial gains observed in the 512+256 setting with the Phi-3.5-4B model. Improvements are significantly stronger on datacenter-grade GPUs like the NVIDIA H100 and more modest on consumer hardware (e.g., Apple M1).

Table 5: **Throughput (tokens/sec)** comparison of the zip2zip framework against the baseline HuggingFace Transformers generate and MLX generate implementation. Performance is detailed for prefilling and decode phases across various context lengths (first value in column headers) combined with a 256-token generation length. zip2zip demonstrates notable throughput improvements, in both the prefilling and decoding phases.

Setting	Method	256+256		512+256		1024+256		2048+256	
		Prefill	Decode	Prefill	Decode	Prefill	Decode	Prefill	Decode
<i>Hardware: Apple M1 (16GB RAM)</i>									
Phi-3.5-4B	Base model	165.0	7.3	211.3	7.5	200.9	7.1	196.6	6.8
	zip2zip	145.5	7.9	231.4	10.1	189.6	7.4	233.8	7.3
	Relative %	-11.8%	+7.5%	+9.5%	+34.8%	-6.6%	+3.9%	+18.9%	+7.5%
<i>Hardware: NVIDIA H100 80GB GPU</i>									
Phi-3.5-4B	Base model	700.9	56.2	1347.2	54.4	2689.4	52.8	4993.2	53.1
	zip2zip	936.6	61.4	2722.1	79.8	4326.7	61.5	9258.1	61.9
	Relative %	+33.6%	+9.3%	+102.6%	+46.6%	+60.9%	+16.6%	+85.4%	+16.5%
Phi-3-14B	Base model	724.4	44.6	1356.3	43.8	2328.6	45.1	3849.5	42.2
	zip2zip	1024.6	54.9	1973.0	61.1	3657.0	66.8	7239.1	46.3
	Relative %	+41.5%	+23.0%	+45.5%	+39.5%	+57.0%	+48.1%	+88.1%	+9.6%

Efficient LZW-Tokenizer Implementation. zip2zip introduces an additional LZW compression step during inference and a decompression step at the end of generation. As a result, the efficiency of LZW-integrated tokenization is important to overall performance. To minimize overhead, we implemented a Rust-based zip2zip tokenizer that outperforms the Python version (see Figure 7) and matches the latency of HuggingFace’s fast BPE tokenizer.

4 Related Work

Domain-Adapted Tokenizers. Several works have explored tokenizer adaptation by expanding the token vocabulary to better support specific domains or languages. Zhao et al. [2024], Kim et al. [2024], Liu et al. [2023, 2024a] adapt the Llama tokenizer to Chinese, Korean, and specialized domains such as mental health and law by adding new tokens. However, these approaches yield a fixed vocabulary that does not adapt during inference.

Input Compression for LLMs. Prompt compression methods such as gist tokens [Mu et al., 2023], selective context [Li et al., 2023], LLMingua [Jiang et al., 2023], summary vectors [Chevalier et al., 2023], in-context autoencoders [Ge et al., 2024], and others [Wingate et al., 2022] reduce the context length by lossy compression. While their lossy compression nature enables high compression ratios, these prompt compression methods can only compress input tokens, but not the output tokens, although output tokens typically dominate generation time under low-batch workloads. Lester et al. [2024] propose improving language model efficiency by training LLMs directly on text compressed with arithmetic coding.

Transformers with Dynamic Embeddings. Architecture-wise, zip2zip employs a dynamic embedding layer built upon transformer blocks. Similar ideas have been explored in prior work aimed at reducing the computational cost of transformers, including Hourglass [Nawrot et al., 2022], dynamic-pooling transformer [Nawrot et al., 2023], MegaByte [Yu et al., 2023], Toucan [Fleshman and Durme, 2023], Learn-Your-Token [Thawani et al., 2023], SpaceByte [Slagle, 2024], ZeTT [Minixhofer et al., 2024], dynamic tokenization [Feher et al., 2025], BLT [Pagnoni et al., 2025], and H-Net [Hwang et al., 2025]. These approaches vary in their model architectures and chunking strategies. Dynamic Vocab [Liu et al., 2024b] is probably the closest in terms of conceptual motivation, as it also expands the vocabulary dynamically during generation. The main difference lies in the dynamic vocabulary construction algorithm and the model training procedure.

5 Discussion and Limitations

Beyond LZW. While we adopt LZW for dynamic construction of hypertokens, zip2zip is broadly compatible with any online compression algorithm. Future work may explore alternative schemes that provide different trade-offs between compression efficiency and model performance.

Codebook Management Strategy. The LZW algorithm grows the codebook linearly with the number of tokens in the context window. Empirical results show that only about 25% of hypertokens are reused during generation, leaving substantial room for optimization. Two potential improvements are (1) *pruning* or *selective retention* strategies to reduce unused entries, and (2) *codebook prefilling*, which could be beneficial if likely tokens can be speculated ahead of input processing.

Optimization Under Lossless Compression. Since zip2zip employs lossless compression, the achievable performance is theoretically invariant under the transformation: a *transported model*, as described in Section 2.6, can attain identical likelihood to that in the original space. Empirically, however, we observe a mild increase in perplexity under compression (Table 3), indicating that the trained model does not perfectly recover the *transported model*. This discrepancy arises from optimization challenges rather than representational limits—gradient descent may converge more slowly or settle in suboptimal regions due to more complex loss landscape. Understanding this optimization difficulty—how the search landscape changes under compression and whether targeted preconditioning or extended training budgets can close the gap—remains an important question for future work.

6 Conclusion

We presented zip2zip, an approach that brings inference-time tokenization to large language models through online token compression. By combining LZW-based sequence compression with dynamic hypertoken embeddings, zip2zip enables compact, adaptive tokenization with lightweight uptraining and little architectural changes. Across multiple domains and languages, it achieves substantial reductions in sequence length and decoding cost while maintaining strong task performance. These results demonstrate that online token compression can serve as a practical path toward dynamic tokenization, pointing to new directions for efficient and adaptable LLM inference.

Acknowledgements

We would like to thank Miao Xiong for proof-reading the paper and providing valuable feedback. We are also grateful to Emre Kiciman, Jason Eisner, Barun Patra, Ana-Maria Andreias, Xiuying Wei, Julian Minder, Tiago Pimental, Luca Beurer-Kellner, and Aleksei Kudrinskii for their helpful

input and insightful discussions throughout this project. Special thanks to Zheng Zhou for providing technical support with the computing infrastructure.

West’s lab is partly supported by grants from Swiss National Science Foundation (TMSGI2_211379 and Grant 200364), Swiss Data Science Center (P22_08), H2020 (952215), Microsoft Swiss Joint Research Center, and Google, and by generous gifts from Facebook, Google, and Microsoft.

References

- Marah Abdin, Jyoti Aneja, Harkirat Behl, Sébastien Bubeck, Ronen Eldan, Suriya Gunasekar, Michael Harrison, Russell J. Hewett, Mojan Javaheripi, Piero Kauffmann, James R. Lee, Yin Tat Lee, Yuanzhi Li, Weishung Liu, Caio C. T. Mendes, Anh Nguyen, Eric Price, Gustavo de Rosa, Olli Saarikivi, Adil Salim, Shital Shah, Xin Wang, Rachel Ward, Yue Wu, Dingli Yu, Cyril Zhang, and Yi Zhang. Phi-4 technical report, 2024. URL <https://arxiv.org/abs/2412.08905>.
- Orevaoghene Ahia, Sachin Kumar, Hila Gonen, Jungo Kasai, David Mortensen, Noah Smith, and Yulia Tsvetkov. Do all languages cost the same? tokenization in the era of commercial language models. In Houda Bouamor, Juan Pino, and Kalika Bali, editors, *Proceedings of the 2023 Conference on Empirical Methods in Natural Language Processing*, pages 9904–9923, Singapore, December 2023. Association for Computational Linguistics. doi: 10.18653/v1/2023.emnlp-main.614. URL <https://aclanthology.org/2023.emnlp-main.614/>.
- Yonatan Bisk, Rowan Zellers, Ronan Le Bras, Jianfeng Gao, and Yejin Choi. Piqa: Reasoning about physical commonsense in natural language. In *AAAI Conference on Artificial Intelligence*, 2019. URL <https://api.semanticscholar.org/CorpusID:208290939>.
- Ondřej Bojar, Rajen Chatterjee, Christian Federmann, Yvette Graham, Barry Haddow, Matthias Huck, Antonio Jimeno Yepes, Philipp Koehn, Varvara Logacheva, Christof Monz, Matteo Negri, Aurélie Névéal, Mariana Neves, Martin Popel, Matt Post, Raphael Rubino, Carolina Scarton, Lucia Specia, Marco Turchi, Karin Verspoor, and Marcos Zampieri. Findings of the 2016 conference on machine translation. In Ondřej Bojar, Christian Buck, Rajen Chatterjee, Christian Federmann, Liane Guillou, Barry Haddow, Matthias Huck, Antonio Jimeno Yepes, Aurélie Névéal, Mariana Neves, Pavel Pecina, Martin Popel, Philipp Koehn, Christof Monz, Matteo Negri, Matt Post, Lucia Specia, Karin Verspoor, Jörg Tiedemann, and Marco Turchi, editors, *Proceedings of the First Conference on Machine Translation: Volume 2, Shared Task Papers*, pages 131–198, Berlin, Germany, August 2016. Association for Computational Linguistics. doi: 10.18653/v1/W16-2301. URL <https://aclanthology.org/W16-2301/>.
- Tom Brown, Benjamin Mann, Nick Ryder, Melanie Subbiah, Jared D Kaplan, Prafulla Dhariwal, Arvind Neelakantan, Pranav Shyam, Girish Sastry, Amanda Askell, Sandhini Agarwal, Ariel Herbert-Voss, Gretchen Krueger, Tom Henighan, Rewon Child, Aditya Ramesh, Daniel Ziegler, Jeffrey Wu, Clemens Winter, Chris Hesse, Mark Chen, Eric Sigler, Mateusz Litwin, Scott Gray, Benjamin Chess, Jack Clark, Christopher Berner, Sam McCandlish, Alec Radford, Ilya Sutskever, and Dario Amodei. Language models are few-shot learners. In H. Larochelle, M. Ranzato, R. Hadsell, M.F. Balcan, and H. Lin, editors, *Advances in Neural Information Processing Systems*, volume 33, pages 1877–1901. Curran Associates, Inc., 2020. URL https://proceedings.neurips.cc/paper_files/paper/2020/file/1457c0d6bfc4967418bfb8ac142f64a-Paper.pdf.
- Sébastien Bubeck, Varun Chandrasekaran, Ronen Eldan, Johannes Gehrike, Eric Horvitz, Ece Kamar, Peter Lee, Yin Tat Lee, Yuanzhi Li, Scott Lundberg, Harsha Nori, Hamid Palangi, Marco Tulio Ribeiro, and Yi Zhang. Sparks of artificial general intelligence: Early experiments with gpt-4, 2023. URL <https://arxiv.org/abs/2303.12712>.
- Alexis Chevalier, Alexander Wettig, Anirudh Ajith, and Danqi Chen. Adapting language models to compress contexts. In Houda Bouamor, Juan Pino, and Kalika Bali, editors, *Proceedings of the 2023 Conference on Empirical Methods in Natural Language Processing*, pages 3829–3846, Singapore, December 2023. Association for Computational Linguistics. doi: 10.18653/v1/2023.emnlp-main.232. URL <https://aclanthology.org/2023.emnlp-main.232/>.
- Peter Clark, Isaac Cowhey, Oren Etzioni, Tushar Khot, Ashish Sabharwal, Carissa Schoenick, and Oyvind Tafjord. Think you have solved question answering? try arc, the ai2 reasoning challenge, 2018. URL <https://arxiv.org/abs/1803.05457>.

- Karl Cobbe, Vineet Kosaraju, Mohammad Bavarian, Mark Chen, Heewoo Jun, Lukasz Kaiser, Matthias Plappert, Jerry Tworek, Jacob Hilton, Reiichiro Nakano, Christopher Hesse, and John Schulman. Training verifiers to solve math word problems. 2021. URL <https://arxiv.org/abs/2110.14168>.
- Gautier Dagan, Gabriel Synnaeve, and Baptiste Rozière. Getting the most out of your tokenizer for pre-training and domain adaptation. In *Proceedings of the 41st International Conference on Machine Learning*, ICML'24. JMLR.org, 2024.
- Ning Ding, Yulin Chen, Bokai Xu, Yujia Qin, Shengding Hu, Zhiyuan Liu, Maosong Sun, and Bowen Zhou. Enhancing chat language models by scaling high-quality instructional conversations. In Houda Bouamor, Juan Pino, and Kalika Bali, editors, *Proceedings of the 2023 Conference on Empirical Methods in Natural Language Processing*, pages 3029–3051, Singapore, December 2023. Association for Computational Linguistics. doi: 10.18653/v1/2023.emnlp-main.183. URL <https://aclanthology.org/2023.emnlp-main.183/>.
- Darius Feher, Ivan Vulić, and Benjamin Minixhofer. Retrofitting large language models with dynamic tokenization. In Wanxiang Che, Joyce Nabende, Ekaterina Shutova, and Mohammad Taher Pilehvar, editors, *Proceedings of the 63rd Annual Meeting of the Association for Computational Linguistics (Volume 1: Long Papers)*, pages 29866–29883, Vienna, Austria, July 2025. Association for Computational Linguistics. ISBN 979-8-89176-251-0. doi: 10.18653/v1/2025.acl-long.1444. URL <https://aclanthology.org/2025.acl-long.1444/>.
- William Fleshman and Benjamin Van Durme. Toucan: Token-aware character level language modeling, 2023. URL <https://arxiv.org/abs/2311.08620>.
- Simon Frieder, Luca Pinchetti, Chevalier Chevalier, Ryan-Rhys Griffiths, Tommaso Salvatori, Thomas Lukasiewicz, Philipp Petersen, and Julius Berner. Mathematical capabilities of chatgpt. In A. Oh, T. Naumann, A. Globerson, K. Saenko, M. Hardt, and S. Levine, editors, *Advances in Neural Information Processing Systems*, volume 36, pages 27699–27744. Curran Associates, Inc., 2023. URL https://proceedings.neurips.cc/paper_files/paper/2023/file/58168e8a92994655d6da3939e7cc0918-Paper-Datasets_and_Benchmarks.pdf.
- Leo Gao, Stella Biderman, Sid Black, Laurence Golding, Travis Hoppe, Charles Foster, Jason Phang, Horace He, Anish Thite, Noa Nabeshima, Shawn Presser, and Connor Leahy. The pile: An 800gb dataset of diverse text for language modeling, 2020. URL <https://arxiv.org/abs/2101.00027>.
- Leo Gao, Jonathan Tow, Baber Abbasi, Stella Biderman, Sid Black, Anthony DiPofi, Charles Foster, Laurence Golding, Jeffrey Hsu, Alain Le Noac’h, Haonan Li, Kyle McDonell, Niklas Muennighoff, Chris Ociepa, Jason Phang, Laria Reynolds, Hailey Schoelkopf, Aviya Skowron, Lintang Sutawika, Eric Tang, Anish Thite, Ben Wang, Kevin Wang, and Andy Zou. The language model evaluation harness, 07 2024. URL <https://zenodo.org/records/12608602>.
- Tao Ge, Hu Jing, Lei Wang, Xun Wang, Si-Qing Chen, and Furu Wei. In-context autoencoder for context compression in a large language model. In *The Twelfth International Conference on Learning Representations*, 2024. URL <https://openreview.net/forum?id=uREj4ZuGJE>.
- Leonidas Gee, Leonardo Rigutini, Marco Ernandes, and Andrea Zugarini. Multi-word tokenization for sequence compression. In Mingxuan Wang and Imed Zitouni, editors, *Proceedings of the 2023 Conference on Empirical Methods in Natural Language Processing: Industry Track*, pages 612–621, Singapore, December 2023. Association for Computational Linguistics. doi: 10.18653/v1/2023.emnlp-industry.58. URL <https://aclanthology.org/2023.emnlp-industry.58/>.
- Aaron Grattafiori, Abhimanyu Dubey, et al. The llama 3 herd of models, 2024. URL <https://arxiv.org/abs/2407.21783>.
- Edward J Hu, Yelong Shen, Phillip Wallis, Zeyuan Allen-Zhu, Yuanzhi Li, Shean Wang, Lu Wang, and Weizhu Chen. LoRA: Low-rank adaptation of large language models. In *International Conference on Learning Representations*, 2022. URL <https://openreview.net/forum?id=nZeVKeeFYf9>.
- Sukjun Hwang, Brandon Wang, and Albert Gu. Dynamic chunking for end-to-end hierarchical sequence modeling, 2025. URL <https://arxiv.org/abs/2507.07955>.

- Huiqiang Jiang, Qianhui Wu, Chin-Yew Lin, Yuqing Yang, and Lili Qiu. LLMLingua: Compressing prompts for accelerated inference of large language models. In Houda Bouamor, Juan Pino, and Kalika Bali, editors, *Proceedings of the 2023 Conference on Empirical Methods in Natural Language Processing*, pages 13358–13376, Singapore, December 2023. Association for Computational Linguistics. doi: 10.18653/v1/2023.emnlp-main.825. URL <https://aclanthology.org/2023.emnlp-main.825>.
- Juyong Jiang, Fan Wang, Jiasi Shen, Sungju Kim, and Sunghun Kim. A survey on large language models for code generation, 2024. URL <https://arxiv.org/abs/2406.00515>.
- Jared Kaplan, Sam McCandlish, Tom Henighan, Tom B. Brown, Benjamin Chess, Rewon Child, Scott Gray, Alec Radford, Jeffrey Wu, and Dario Amodei. Scaling laws for neural language models, 2020. URL <https://arxiv.org/abs/2001.08361>.
- Seungduk Kim, Seungtaek Choi, and Myeongho Jeong. Efficient and effective vocabulary expansion towards multilingual large language models, 2024. URL <https://arxiv.org/abs/2402.14714>.
- Brian Lester, Jaehoon Lee, Alexander A Alemi, Jeffrey Pennington, Adam Roberts, Jascha Sohl-Dickstein, and Noah Constant. Training LLMs over neurally compressed text. *Transactions on Machine Learning Research*, 2024. ISSN 2835-8856. URL <https://openreview.net/forum?id=pRvhMSV48t>. Featured Certification.
- Jia LI, Edward Beeching, Lewis Tunstall, Ben Lipkin, Roman Soletskyi, Shengyi Costa Huang, Kashif Rasul, Longhui Yu, Albert Jiang, Ziju Shen, Zihan Qin, Bin Dong, Li Zhou, Yann Fleureau, Guillaume Lample, and Stanislas Polu. NuminaMath. [<https://huggingface.co/AI-M0/NuminaMath-1.5>](https://github.com/project-numina/aimo-progress-prize/blob/main/report/numina_dataset.pdf), 2024.
- Yucheng Li, Bo Dong, Frank Guerin, and Chenghua Lin. Compressing context to enhance inference efficiency of large language models. In Houda Bouamor, Juan Pino, and Kalika Bali, editors, *Proceedings of the 2023 Conference on Empirical Methods in Natural Language Processing*, pages 6342–6353, Singapore, December 2023. Association for Computational Linguistics. doi: 10.18653/v1/2023.emnlp-main.391. URL <https://aclanthology.org/2023.emnlp-main.391/>.
- Davis Liang, Hila Gonen, Yuning Mao, Rui Hou, Naman Goyal, Marjan Ghazvininejad, Luke Zettlemoyer, and Madian Khabza. XLM-V: Overcoming the vocabulary bottleneck in multilingual masked language models. In Houda Bouamor, Juan Pino, and Kalika Bali, editors, *Proceedings of the 2023 Conference on Empirical Methods in Natural Language Processing*, pages 13142–13152, Singapore, December 2023. Association for Computational Linguistics. doi: 10.18653/v1/2023.emnlp-main.813. URL <https://aclanthology.org/2023.emnlp-main.813/>.
- Alisa Liu, Jonathan Hayase, Valentin Hofmann, Sewoong Oh, Noah A Smith, and Yejin Choi. SuperBPE: Space travel for language models. In *Second Conference on Language Modeling*, 2025. URL <https://arxiv.org/abs/2503.13423>.
- Chengyuan Liu, Shihang Wang, Lizhi Qing, Kun Kuang, Yangyang Kang, Changlong Sun, and Fei Wu. Gold panning in vocabulary: An adaptive method for vocabulary expansion of domain-specific LLMs. In Yaser Al-Onaizan, Mohit Bansal, and Yun-Nung Chen, editors, *Proceedings of the 2024 Conference on Empirical Methods in Natural Language Processing*, pages 7442–7459, Miami, Florida, USA, November 2024a. Association for Computational Linguistics. doi: 10.18653/v1/2024.emnlp-main.424. URL <https://aclanthology.org/2024.emnlp-main.424/>.
- Siyang Liu, Naihao Deng, Sahand Sabour, Yilin Jia, Minlie Huang, and Rada Mihalcea. Task-adaptive tokenization: Enhancing long-form text generation efficacy in mental health and beyond. In Houda Bouamor, Juan Pino, and Kalika Bali, editors, *Proceedings of the 2023 Conference on Empirical Methods in Natural Language Processing*, pages 15264–15281, Singapore, December 2023. Association for Computational Linguistics. doi: 10.18653/v1/2023.emnlp-main.944. URL <https://aclanthology.org/2023.emnlp-main.944/>.
- Yanting Liu, Tao Ji, Changzhi Sun, Yuanbin Wu, and Xiaoling Wang. Generation with dynamic vocabulary. In Yaser Al-Onaizan, Mohit Bansal, and Yun-Nung Chen, editors, *Proceedings of the 2024 Conference on Empirical Methods in Natural Language Processing*, pages 18931–18948, Miami, Florida, USA, November 2024b. Association for Computational Linguistics. doi: 10.18653/v1/2024.emnlp-main.1053. URL <https://aclanthology.org/2024.emnlp-main.1053/>.

- Jonas F. Lotz, Hendra Setiawan, Stephan Peitz, and Yova Kementchedjhieva. Overcoming vocabulary constraints with pixel-level fallback, 2025. URL <https://arxiv.org/abs/2504.02122>.
- Anton Lozhkov, Loubna Ben Allal, Leandro von Werra, and Thomas Wolf. Fineweb-edu: the finest collection of educational content, 2024a. URL <https://huggingface.co/datasets/HuggingFaceFW/fineweb-edu>.
- Anton Lozhkov, Raymond Li, et al. Starcoder 2 and the stack v2: The next generation, 2024b.
- Matouš Macháček and Ondřej Bojar. Results of the WMT14 metrics shared task. In Ondřej Bojar, Christian Buck, Christian Federmann, Barry Haddow, Philipp Koehn, Christof Monz, Matt Post, and Lucia Specia, editors, *Proceedings of the Ninth Workshop on Statistical Machine Translation*, pages 293–301, Baltimore, Maryland, USA, June 2014. Association for Computational Linguistics. doi: 10.3115/v1/W14-3336. URL <https://aclanthology.org/W14-3336/>.
- Ian Magnusson, Akshita Bhagia, Valentin Hofmann, Luca Soldaini, A. Jha, Oyvind Tafjord, Dustin Schwenk, Pete Walsh, Yanai Elazar, Kyle Lo, Dirk Groeneveld, Iz Beltagy, Hanna Hajishirzi, Noah A. Smith, Kyle Richardson, and Jesse Dodge. Paloma: A benchmark for evaluating language model fit. *ArXiv*, abs/2312.10523, 2023. URL <https://api.semanticscholar.org/CorpusID:266348815>.
- Stephen Merity, Caiming Xiong, James Bradbury, and Richard Socher. Pointer sentinel mixture models, 2016. URL <https://arxiv.org/abs/1609.07843>.
- Todor Mihaylov, Peter Clark, Tushar Khot, and Ashish Sabharwal. Can a suit of armor conduct electricity? a new dataset for open book question answering. In Ellen Riloff, David Chiang, Julia Hockenmaier, and Jun’ichi Tsujii, editors, *Proceedings of the 2018 Conference on Empirical Methods in Natural Language Processing*, pages 2381–2391, Brussels, Belgium, October–November 2018. Association for Computational Linguistics. doi: 10.18653/v1/D18-1260. URL <https://aclanthology.org/D18-1260/>.
- Benjamin Minixhofer, Edoardo M. Ponti, and Ivan Vulić. Zero-shot tokenizer transfer. In A. Globerson, L. Mackey, D. Belgrave, A. Fan, U. Paquet, J. Tomczak, and C. Zhang, editors, *Advances in Neural Information Processing Systems*, volume 37, pages 46791–46818. Curran Associates, Inc., 2024. URL https://proceedings.neurips.cc/paper_files/paper/2024/file/532ce4fcf853023c4cf2ac38cbc5d002-Paper-Conference.pdf.
- Jesse Mu, Xiang Li, and Noah Goodman. Learning to compress prompts with gist tokens. In A. Oh, T. Naumann, A. Globerson, K. Saenko, M. Hardt, and S. Levine, editors, *Advances in Neural Information Processing Systems*, volume 36, pages 19327–19352. Curran Associates, Inc., 2023. URL https://proceedings.neurips.cc/paper_files/paper/2023/file/3d77c6dcc7f143aa2154e7f4d5e22d68-Paper-Conference.pdf.
- Piotr Nawrot, Szymon Tworowski, Michał Tyrolski, Lukasz Kaiser, Yuhuai Wu, Christian Szegedy, and Henryk Michalewski. Hierarchical transformers are more efficient language models. In Marine Carpuat, Marie-Catherine de Marneffe, and Ivan Vladimir Meza Ruiz, editors, *Findings of the Association for Computational Linguistics: NAACL 2022*, pages 1559–1571, Seattle, United States, July 2022. Association for Computational Linguistics. doi: 10.18653/v1/2022.findings-naacl.117. URL <https://aclanthology.org/2022.findings-naacl.117/>.
- Piotr Nawrot, Jan Chorowski, Adrian Lancucki, and Edoardo Maria Ponti. Efficient transformers with dynamic token pooling. In Anna Rogers, Jordan Boyd-Graber, and Naoaki Okazaki, editors, *Proceedings of the 61st Annual Meeting of the Association for Computational Linguistics (Volume 1: Long Papers)*, pages 6403–6417, Toronto, Canada, July 2023. Association for Computational Linguistics. doi: 10.18653/v1/2023.acl-long.353. URL <https://aclanthology.org/2023.acl-long.353/>.
- Harsha Nori, Nicholas King, Scott Mayer McKinney, Dean Carignan, and Eric Horvitz. Capabilities of gpt-4 on medical challenge problems, 2023. URL <https://arxiv.org/abs/2303.13375>.
- Abraham Toluwase Owodunni, Orevaoghene Ahia, and Sachin Kumar. Flexitokens: Flexible tokenization for evolving language models, 2025. URL <https://arxiv.org/abs/2507.12720>.

- Artidoro Pagnoni, Ramakanth Pasunuru, Pedro Rodriguez, John Nguyen, Benjamin Muller, Margaret Li, Chunting Zhou, Lili Yu, Jason E Weston, Luke Zettlemoyer, Gargi Ghosh, Mike Lewis, Ari Holtzman, and Srini Iyer. Byte latent transformer: Patches scale better than tokens. In Wanxiang Che, Joyce Nabende, Ekaterina Shutova, and Mohammad Taher Pilehvar, editors, *Proceedings of the 63rd Annual Meeting of the Association for Computational Linguistics (Volume 1: Long Papers)*, pages 9238–9258, Vienna, Austria, July 2025. Association for Computational Linguistics. ISBN 979-8-89176-251-0. doi: 10.18653/v1/2025.acl-long.453. URL <https://aclanthology.org/2025.acl-long.453/>.
- Denis Paperno, Germán Kruszewski, Angeliki Lazaridou, Ngoc Quan Pham, Raffaella Bernardi, Sandro Pezzelle, Marco Baroni, Gemma Boleda, and Raquel Fernández. The LAMBADA dataset: Word prediction requiring a broad discourse context. In Katrin Erk and Noah A. Smith, editors, *Proceedings of the 54th Annual Meeting of the Association for Computational Linguistics (Volume 1: Long Papers)*, pages 1525–1534, Berlin, Germany, August 2016. Association for Computational Linguistics. doi: 10.18653/v1/P16-1144. URL <https://aclanthology.org/P16-1144/>.
- Guilherme Penedo, Hynek Kydlíček, Vinko Sabolčec, Bettina Messmer, Negar Foroutan, Martin Jaggi, Leandro von Werra, and Thomas Wolf. Fineweb2: A sparkling update with 1000s of languages, 2024. URL <https://huggingface.co/datasets/HuggingFaceFW/fineweb-2>.
- Aleksandar Petrov, Emanuele La Malfa, Philip H. S. Torr, and Adel Bibi. Language model tokenizers introduce unfairness between languages. In *Advances in Neural Information Processing Systems*, 2023. URL <https://arxiv.org/abs/2305.15425>.
- Alec Radford, Jeff Wu, Rewon Child, David Luan, Dario Amodei, and Ilya Sutskever. Language models are unsupervised multitask learners. *OpenAI blog*, 2019. URL <https://api.semanticscholar.org/CorpusID:160025533>.
- Keisuke Sakaguchi, Ronan Le Bras, Chandra Bhagavatula, and Yejin Choi. Winogrande. *Communications of the ACM*, 64:99 – 106, 2019. URL <https://api.semanticscholar.org/CorpusID:198893658>.
- Rico Sennrich, Barry Haddow, and Alexandra Birch. Neural machine translation of rare words with subword units. In Katrin Erk and Noah A. Smith, editors, *Proceedings of the 54th Annual Meeting of the Association for Computational Linguistics (Volume 1: Long Papers)*, pages 1715–1725, Berlin, Germany, August 2016. Association for Computational Linguistics. doi: 10.18653/v1/P16-1162. URL <https://aclanthology.org/P16-1162/>.
- Junhong Shen, Kushal Tirumala, Michihiro Yasunaga, Ishan Misra, Luke Zettlemoyer, Lili Yu, and Chunting Zhou. Cat: Content-adaptive image tokenization, 2025. URL <https://arxiv.org/abs/2501.03120>.
- Aaditya K. Singh and DJ Strouse. Tokenization counts: the impact of tokenization on arithmetic in frontier llms, 2024. URL <https://arxiv.org/abs/2402.14903>.
- Kevin Slagle. Spacebyte: Towards deleting tokenization from large language modeling. In *Proceedings of the 38th Conference on Neural Information Processing Systems (NeurIPS 2024)*, 2024. URL https://proceedings.neurips.cc/paper_files/paper/2024/file/e1f418450107c4a0ddc16d008d131573-Paper-Conference.pdf.
- Ilya Sutskever, Oriol Vinyals, and Quoc V. Le. Sequence to sequence learning with neural networks. In *Proceedings of the 28th International Conference on Neural Information Processing Systems - Volume 2*, NIPS’14, page 3104–3112, Cambridge, MA, USA, 2014. MIT Press.
- Gemma Team. Gemma 3 technical report, 2025. URL <https://arxiv.org/abs/2503.19786>.
- Avijit Thawani, Saurabh Ghanekar, Xiaoyuan Zhu, and Jay Pujara. Learn your tokens: Word-pooled tokenization for language modeling. In Houda Bouamor, Juan Pino, and Kalika Bali, editors, *Findings of the Association for Computational Linguistics: EMNLP 2023*, pages 9883–9893, Singapore, December 2023. Association for Computational Linguistics. doi: 10.18653/v1/2023.findings-emnlp.662. URL <https://aclanthology.org/2023.findings-emnlp.662/>.

- Ashish Vaswani, Noam Shazeer, Niki Parmar, Jakob Uszkoreit, Llion Jones, Aidan N Gomez, Łukasz Kaiser, and Illia Polosukhin. Attention is all you need. In I. Guyon, U. Von Luxburg, S. Bengio, H. Wallach, R. Fergus, S. Vishwanathan, and R. Garnett, editors, *Advances in Neural Information Processing Systems*, volume 30. Curran Associates, Inc., 2017. URL https://proceedings.neurips.cc/paper_files/paper/2017/file/3f5ee243547dee91fbd053c1c4a845aa-Paper.pdf.
- Hai Wang, Dian Yu, Kai Sun, Jianshu Chen, and Dong Yu. Improving pre-trained multilingual model with vocabulary expansion. In Mohit Bansal and Aline Villavicencio, editors, *Proceedings of the 23rd Conference on Computational Natural Language Learning (CoNLL)*, pages 316–327, Hong Kong, China, November 2019. Association for Computational Linguistics. doi: 10.18653/v1/K19-1030. URL <https://aclanthology.org/K19-1030/>.
- Shumin Wang, Yuexiang Xie, Bolin Ding, Jinyang Gao, and Yanyong Zhang. Language adaptation of large language models: An empirical study on LLaMA2. In Owen Rambow, Leo Wanner, Marianna Apidianaki, Hend Al-Khalifa, Barbara Di Eugenio, and Steven Schockaert, editors, *Proceedings of the 31st International Conference on Computational Linguistics*, pages 7195–7208, Abu Dhabi, UAE, January 2025. Association for Computational Linguistics. URL <https://aclanthology.org/2025.coling-main.480/>.
- Welch. A technique for high-performance data compression. *Computer*, 17(6):8–19, 1984. doi: 10.1109/MC.1984.1659158.
- David Wingate, Mohammad Shoeybi, and Taylor Sorensen. Prompt compression and contrastive conditioning for controllability and toxicity reduction in language models. In Yoav Goldberg, Zornitsa Kozareva, and Yue Zhang, editors, *Findings of the Association for Computational Linguistics: EMNLP 2022*, pages 5621–5634, Abu Dhabi, United Arab Emirates, December 2022. Association for Computational Linguistics. doi: 10.18653/v1/2022.findings-emnlp.412. URL <https://aclanthology.org/2022.findings-emnlp.412/>.
- An Yang, Baosong Yang, et al. Qwen2 technical report, 2024. URL <https://arxiv.org/abs/2407.10671>.
- Lili Yu, Daniel Simig, Colin Flaherty, Armen Aghajanyan, Luke Zettlemoyer, and Mike Lewis. Megabyte: Predicting million-byte sequences with multiscale transformers. In *Proceedings of the 37th Conference on Neural Information Processing Systems (NeurIPS 2023)*, 2023. URL <https://neurips.cc/virtual/2023/poster/71722>.
- Rowan Zellers, Ari Holtzman, Yonatan Bisk, Ali Farhadi, and Yejin Choi. HellaSwag: Can a machine really finish your sentence? In Anna Korhonen, David Traum, and Lluís Màrquez, editors, *Proceedings of the 57th Annual Meeting of the Association for Computational Linguistics*, pages 4791–4800, Florence, Italy, July 2019. Association for Computational Linguistics. doi: 10.18653/v1/P19-1472. URL <https://aclanthology.org/P19-1472/>.
- Jun Zhao, Zhihao Zhang, Luhui Gao, Qi Zhang, Tao Gui, and Xuanjing Huang. Llama beyond english: An empirical study on language capability transfer, 2024. URL <https://arxiv.org/abs/2401.01055>.

A More Related Work

Wang et al. [2025], Liu et al. [2024a] conducted studies on how to effectively expand the vocabulary by better selecting the subset of tokens to add. Multi-Word Tokenizer [Gee et al., 2023] and SuperBPE [Liu et al., 2025] demonstrated that allowing forming tokens beyond word boundaries in BPE vocab learning helps to achieve more compact tokenization and even improves model performance. Content-Adaptive Tokenizer (CAT) by [Shen et al., 2025] introduces a dynamic image tokenization approach that allocates tokens based on content complexity, achieving improved reconstruction quality and efficiency compared to fixed-size tokenization methods. [Lotz et al., 2025] propose a pixel-level fallback encoder that bypasses subword vocabulary limitations by rendering text as images, enabling vocabulary-free representations that improve multilingual performance and efficiency in pretrained language models. The FlexiTokens [Owodunni et al., 2025] introduces learnable, byte-level tokenizers that dynamically adapt token boundaries to new domains and languages, reducing over-fragmentation.

B Discussions on Merge Size

B.1 An Upper Bound on Merge Size

Proposition B.1. *Let T be an input sequence of length N over a finite alphabet. LZW compression algorithm merges substrings by identifying and replacing the most frequent substrings with new symbols, iteratively. Then, the size M of the largest merged unit (i.e., the longest substring created via merging) is bounded above by $O(\sqrt{N})$.*

Proof. Assume that the largest merged unit has size M . This implies that there exists at least one merge at level M involving a substring of length M . Furthermore, due to the nature of merge-based algorithms, any merged unit of size k must be composed of previously merged units of smaller sizes (e.g., from sizes $k - 1$ and 1, or similar). Hence, in order to construct a merged unit of size M , the algorithm must have previously created all merged units of sizes 1 through $M - 1$.

Thus, the existence of a merged unit of size M implies the existence of merged units of every size k such that $1 \leq k \leq M$. Each such unit must occur at least once in the input sequence in order to be merged.

Therefore, the total number of characters in T must be at least the sum of the lengths of all merged units from size 1 to M , i.e.,

$$N \geq \sum_{k=1}^M k = \frac{M(M+1)}{2}.$$

This implies:

$$M = O(\sqrt{N}).$$

Thus, the length M of the largest merged unit is bounded above by $O(\sqrt{N})$. \square

B.2 Relation Between Merge Size and Compression Rate

Definition B.1 (Compression Rate). *We define the compression rate as the ratio between the number of tokens after compression (N_{comp}) and the number of tokens in the original uncompressed text (N_{orig}), expressed as a percentage:*

$$\text{Compression Rate} = \frac{N_{comp}}{N_{orig}} \times 100\%.$$

A lower compression rate indicates greater reduction in token count, and thus more effective compression.

The last column of Table 6 shows how the maximum merge size M affects compression rate when the context window length is 2048. As M increases, compression rate improves significantly, especially from $M = 1$ to $M = 3$. Beyond that, gains diminish, suggesting $M = 3$ strikes a good balance between efficiency and compression rate.

Table 6: **Effect of maximum merge size (M) on byte-level perplexity and compression rate.** Perplexity is measured for Phi-3.5-4B across four corpora with a 1024-token context window. Compression rate is evaluated over the training corpus with a 2048-token context. $M = 1$ corresponds to no compression.

M	Wiki	Pile	mC4	dC4	Compression Rate(%)
1	1.62	1.70	2.00	1.91	100.00
2	1.96	2.21	2.55	2.22	75.30
3	1.72	1.84	2.15	2.00	71.21
4	1.71	1.84	2.14	1.99	68.93
5	1.72	1.84	2.14	1.99	68.41

Interestingly, the relationship between maximum merge size and training loss in Figure 5 as well as perplexity in Table 6 is non-monotonic. The baseline case with $M = 1$ (i.e., no zip2zip compression) yields the lowest perplexity overall, which is expected and consistent with prior findings that

Table 7: **Ablation of hyper-encoder architecture** on byte-perplexity (\downarrow) across four corpora using a 1024-token context window. Performance improves with increasingly expressive architectures.

Model	Method	Wiki	Pile	mC4	dC4
Phi-3.5-4B	averaging	1.81	1.97	2.29	2.08
	1-attention-layer	1.73	1.86	2.16	2.01
	1-transformer-layer	1.71	1.83	2.13	1.99
	2-transformer-layer	1.72	1.84	2.15	2.00

compression typically incurs a trade-off in model performance. Among the compressed settings, the case $M = 2$ performs the worst, with noticeably slower convergence and higher final loss. In contrast, the case $M = 3$ achieves the best performance within the compressed configurations, striking a favorable balance between compression and prediction performance. While $M = 4$ and $M = 5$ also perform reasonably well, they exhibit slightly higher loss than $M = 3$, suggesting diminishing returns or possible over-compression at larger maximum merge sizes (see Figure 5).

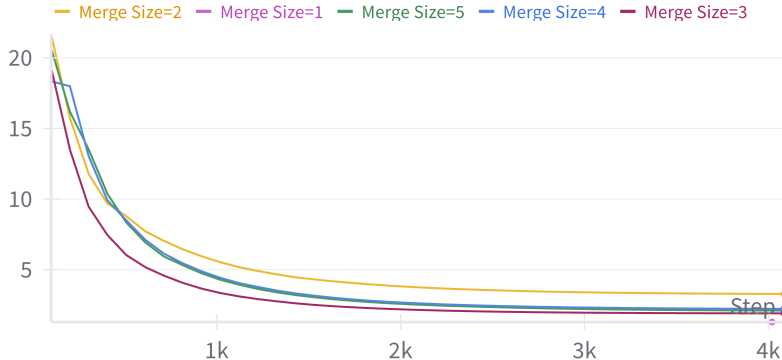


Figure 5: **Effect of maximum merge size M on zip2zip training loss:** $M = 1$ (no compression) achieves the lowest loss overall. Among compressed settings, $M = 3$ performs best, while $M = 2$ shows the worst convergence. Larger M (4 and 5) yield slightly worse results than $M = 3$.

Table 6 reports the byte-level perplexity across four corpora using a 1024-token context window. The results align closely with the training loss trends observed earlier. Setting $M = 1$ (i.e., no compression) consistently achieves the lowest perplexity across all datasets, reaffirming that compression introduces a performance trade-off. Notably, $M = 2$ performs the worst across all corpora, exhibiting the highest perplexity values. For merge sizes $M = 3$, $M = 4$, and $M = 5$, perplexity scores are nearly identical, suggesting that moderate compression can be achieved without significantly sacrificing language modeling quality—provided $M = 2$ is avoided. This consistency across loss and perplexity metrics further supports the robustness of maximum merge size $M = 3$ as the most effective trade-off point.

C Discussions on Hyper-Encoder Architecture

C.1 Hyper-encoder architecture

We ablate the architecture of the hyper-encoder to evaluate its effect on language modeling performance, as shown in Table 7. We compare increasingly expressive architectures, starting with a simple averaging method that introduces no additional parameters. This baseline yields the highest perplexity, highlighting its limited capacity. Adding a single attention layer significantly improves performance, and further gains are observed with a 1-layer transformer encoder. The 2-layer transformer offers marginal additional benefit, suggesting that a lightweight transformer (1–2 layers) is sufficient for effective hypertoken modeling.

Figure 6 illustrates the effect of hyper-encoder architecture on zip2zip training loss. We observe that the simple averaging method converges the fastest but plateaus at a relatively high loss, reflecting its limited capacity. As model complexity increases—with attention and transformer layers—the convergence becomes slower, yet the final loss is significantly lower. Notably, the 1-layer and 2-layer

transformer encoders yield the best performance, demonstrating that additional parameters enable the model to better capture structure, albeit at the cost of slower training dynamics.

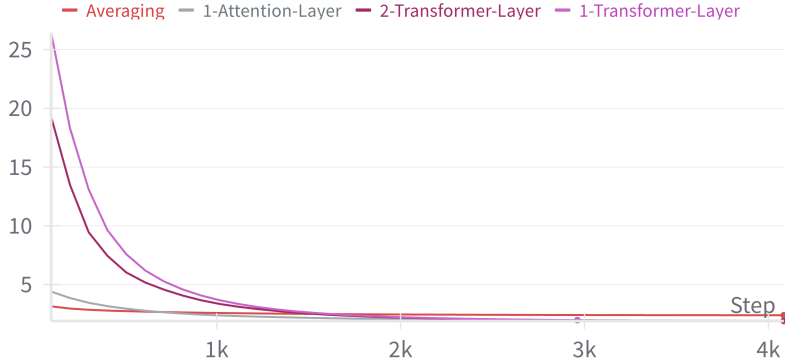


Figure 6: **Effect of hyper-encoder architecture on zip2zip training loss.** Averaging (no additional parameters) converges quickly but to a higher loss. As architectural complexity increases—from attention to transformer layers—convergence becomes slower, but the final loss is lower. This highlights a trade-off between training speed and modeling capacity.

D Discussions on Compression

Table 8: Token statistics for Code Generation, Biomedical, and French QA domains.

Stats	Code	Biomedical	French
Original Seq Len	344	322	399
Zip2Zip Seq Len	265	270	367
Num Hypertoken	44	35	26
Hypertoken Ratio	0.166	0.130	0.071
Compression Rate	0.770	0.839	0.920

Table 8 shows detailed token statistics on illustrative examples across three domains in Figure 4, highlighting zip2zip’s ability to reduce sequence length and introduce reusable hypertokens with domain-specific efficiency.

Table 9: **Sequence length reduction (%)** across domains, inferred from the inverse of token efficiency gains in Table 2.

Tokenizer	Code	Math	Chat	Multilingual	Web
Llama-3-128K	34.9%	32.5%	20.3%	19.1%	14.8%
Qwen-2-150K	35.5%	37.8%	20.3%	19.6%	15.4%
Phi-4-200K	34.9%	34.1%	19.4%	16.4%	13.0%
Gemma-3-256K	41.1%	37.8%	21.9%	18.5%	16.7%

Table 9 reports the estimated sequence length reduction across domains, showing that zip2zip consistently shortens token sequences by 13–41%, with the strongest gains observed in structured domains like code and math.

E FLOPs Estimation for zip2zip

Following the assumptions of Kaplan et al. [2020], we estimate training FLOPs (Γ) as:

$$\Gamma \approx 6 \cdot N_{\text{tokens}} \cdot N_{\text{params}},$$

where N_{tokens} is the total number of processed tokens and N_{params} is the number of trainable parameters. This estimate ignores the quadratic attention cost, assuming:

$12 \cdot d_{\text{model}} \ll \text{sequence length}$.

For zip2zip, this becomes:

$$\Gamma_{z2z} \approx 6 \cdot N_{\text{tokens}} \cdot \rho \cdot N_{\text{params}}(1 + \alpha),$$

where ρ is the compression ratio, and α accounts for the overhead of the hyper-encoder applied at the embedding and LM head. The relative FLOPs ratio is then:

$$\frac{\Gamma_{z2z}}{\Gamma} = \rho \cdot (1 + \alpha).$$

Assuming the hyper-encoder mirrors the base model’s configuration, we estimate:

$$\alpha \approx \frac{lM}{L},$$

where l is the number of hyper-encoder layers, M is the maximum merge size, and L is the number of base model layers. We illustrate this estimate across several model scales in Table 10, showing that the relative FLOPs overhead from the hyper-module remains modest (typically under 15%).

Model	L	M	l	$\alpha = \frac{lM}{L}$
Transformer-4B	14	2	1	0.14
Transformer-7B	32	2	2	0.13
Transformer-70B	80	3	3	0.11
Transformer-400B	128	3	4	0.09

Table 10: Relative FLOPs overhead from the hyper-module across different model sizes.

F Discussions on Tokenizer

Figure 7 compares the tokenization and detokenization latencies across different tokenizer configurations. The Base Tokenizer corresponds to the standard BPE tokenizer implemented by the Hugging Face tokenizers library. The Rust LZW Tokenizer represents the end-to-end latency when LZW compression and decompression are applied on top of the BPE tokenization. As shown, this configuration introduces only a small additional latency in the tokenization process while leaving the detokenization latency virtually unchanged. The Python LZW Tokenizer, in contrast, exhibits significantly higher latency due to Python’s runtime overhead. Overall, the results indicate that most of the observed latency arises from the BPE segmentation process itself rather than the LZW compression, suggesting that efficient implementations of compression add minimal overhead to tokenization workflows.

G Entropy Invariance under Lossless Transformations

Theorem G.1 (Entropy Invariance under Lossless Compression). *Let $g : \mathcal{X}^* \rightarrow \mathcal{Z}^*$ be a bijection onto its image, and let P_Z and p_γ denote the push-forward distributions of P_X and p_θ , respectively:*

$$P_Z(z) = P_X(g^{-1}(z)), \quad p_\gamma(z) = p_\theta(g^{-1}(z)).$$

Then the total entropy and cross-entropy are invariant under g :

$$H(P_Z) = H(P_X), \quad H(P_Z, p_\gamma) = H(P_X, p_\theta).$$

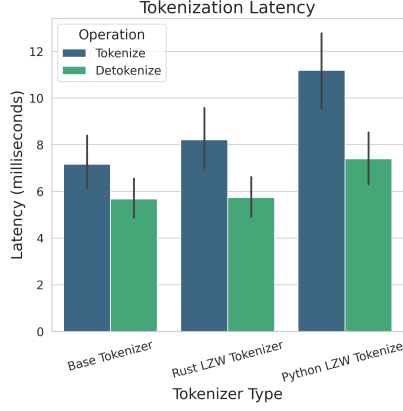


Figure 7: zip2zip tokenizer latency (ms) vs. HF tokenizer.

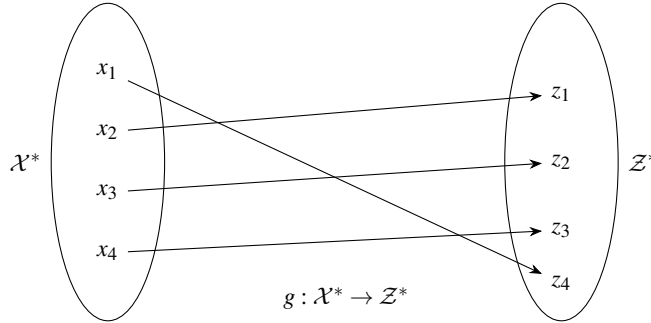


Figure 8: Lossless compression mapping (bijective) g (e.g., LZW) from original sequences \mathcal{X}^* to compressed sequences \mathcal{Z}^* .

Proof. By definition of the push-forward distribution,

$$\begin{aligned}
 H(P_Z) &= - \sum_{z \in \mathcal{Z}^*} P_Z(z) \log P_Z(z) \\
 &= - \sum_{z \in \mathcal{Z}^*} P_X(g^{-1}(z)) \log P_X(g^{-1}(z)) \\
 &= - \sum_{g(x') \in \mathcal{Z}^*} P_X(x') \log P_X(x').
 \end{aligned}$$

Since g is a bijection, we can replace the summation by $x' \in \mathcal{X}^*$, which yields

$$H(P_Z) = - \sum_{x \in \mathcal{X}^*} P_X(x) \log P_X(x) = H(P_X).$$

An identical argument applies to the cross-entropy by considering $P_X(x) \log p_\theta(x)$ as a single function, since the invariance property does not depend on the specific form of the function being summed:

$$\begin{aligned}
 H(P_Z, p_\gamma) &= - \sum_z P_Z(z) \log p_\gamma(z) \\
 &= - \sum_x P_X(x) \log p_\theta(x) = H(P_X, p_\theta).
 \end{aligned}$$

Hence, both entropy and cross-entropy remain invariant under any lossless (bijective) transformation g . \square

H Additional Results

H.1 Machine Translation

We report standard deviations for machine translation results across WMT benchmarks in Table 11, computed using the `lm-evaluation-harness` codebase.

Table 11: Machine translation performance on WMT benchmarks (BLEU \uparrow , CHRF \uparrow , TER \downarrow) with standard deviations (\pm) from bootstrapped estimates. Scores are averaged across both directions.

Model	Method	WMT14 En-Fr			WMT16 En-De			WMT16 En-Ro		
		BLEU	CHRF	TER	BLEU	CHRF	TER	BLEU	CHRF	TER
Phi-3.5-4B	Base	33.6 \pm 2.1	58.3 \pm 1.4	53.0 \pm 1.7	39.2 \pm 1.9	63.2 \pm 1.6	47.9 \pm 1.8	17.7 \pm 1.5	45.5 \pm 1.3	73.4 \pm 2.4
	Cont. pretrain	36.5 \pm 2.2	61.0 \pm 1.6	51.5 \pm 1.8	42.3 \pm 1.8	65.4 \pm 1.4	44.9 \pm 1.7	16.7 \pm 1.4	45.8 \pm 1.5	79.7 \pm 2.3
	zip2zip	34.1 \pm 1.9	59.4 \pm 1.5	54.5 \pm 2.0	39.7 \pm 1.7	64.5 \pm 1.6	48.0 \pm 1.9	14.3 \pm 1.6	44.2 \pm 1.4	93.5 \pm 2.5
Phi-3-14B	Base	39.1 \pm 2.0	62.6 \pm 1.4	49.3 \pm 1.9	43.1 \pm 2.0	65.6 \pm 1.5	44.1 \pm 1.7	21.3 \pm 1.5	51.0 \pm 1.4	70.5 \pm 2.2
	Cont. pretrain	38.9 \pm 2.2	63.2 \pm 1.4	48.8 \pm 1.9	48.4 \pm 2.0	70.1 \pm 1.3	39.8 \pm 1.9	21.8 \pm 1.4	52.0 \pm 1.3	68.3 \pm 2.9
	zip2zip	36.4 \pm 2.1	62.8 \pm 1.5	51.2 \pm 1.8	44.8 \pm 2.1	68.1 \pm 1.6	42.9 \pm 1.8	19.5 \pm 1.5	50.1 \pm 1.3	72.9 \pm 2.6

H.2 Multilingual QA Tasks

We evaluate Phi-3.5-4B on multilingual downstream tasks beyond translation, including TruthfulQA-2, HellaSwag, and Winograd across five languages (French, Spanish, Russian, Chinese, and Arabic). As shown in Table 12, the base model demonstrates strong cross-lingual generalization. Continued pretraining in the vanilla setting slightly reduces performance, likely due to domain drift, while the zip2zip variant performs similarly. Overall, the results indicate that the proposed multilingual adaptation strategy maintains competitive performance across diverse evaluation benchmarks.

Table 12: Evaluation on Multilingual Tasks in addition to Translation. We report results on **TruthfulQA-2**, **HellaSwag**, and **Winograd** across 5 languages (FR, ES, RU, ZH, AR) using `lm-evaluation-harness`.

Model	Method	TruthfulQA-2					HellaSwag					Winograd				
		FR	ES	RU	ZH	AR	FR	ES	RU	ZH	AR	FR	ES	RU	ZH	AR
Phi-3.5-4B	Base	0.47	0.51	0.46	0.41	0.42	0.61	0.66	0.49	NA	0.44	0.70	NA	0.74	0.74	NA
	Cont. Pretrain. Vanilla	0.42	0.47	0.46	0.46	0.43	0.54	0.57	0.37	NA	0.27	0.76	NA	0.70	0.61	NA
	Cont. Pretrain. zip2zip	0.41	0.46	0.47	0.43	0.40	0.55	0.55	0.36	NA	0.27	0.77	NA	0.73	0.64	NA

I Technical Details

I.1 Model and Training Configuration

- **Pretrained Model:** microsoft/Phi-3-medium-4k-instruct
- **Sequence Length:** 1024
- **Total Batch Size:** 32,768 tokens
- **Learning Rate Schedule:** Cosine decay
- **Learning Rate Range:** Max = 3e-4, Min = 1e-5
- **LoRA rank and alpha value:** Both are 32
- **Training Steps:** 10,000
- **Validation Interval:** Every 100 steps
- **Checkpoint Interval:** Every 500 steps
- **Pytorch Model Compilation:** Enabled

I.2 LoRA Configuration

- **Rank:** 16
- **Alpha:** 16
- **Target Modules:** qkv_proj, o_proj, gate_proj, down_proj, up_proj

I.3 Loss Weighting Coefficient

Since both the language modeling loss and the auxiliary reconstruction loss are formulated as cross-entropy objectives over tokens, they are naturally on a comparable scale. For a sequence of N base tokens, the number of hypertokens used in the auto-reconstruction loss is upper-bounded by N , while each hypertoken corresponds to at most M base tokens in the reconstruction target. The loss weighting coefficient λ primarily serves to fine-tune the relative importance of the auxiliary objective rather than to correct for scale mismatch. We set $\lambda = 0.1$, which yielded stable training. We did not perform extensive exploration over the value of λ , which we leave as an interesting direction for future work.

I.4 System and Libraries

- **Hardware:** 4 \times NVIDIA A100-SXM4-80GB GPUs, 64-core CPU (128 threads)
- **Key Libraries:**
 - PyTorch $\geq 2.5.0$
 - Transformers $\geq 4.47.0$
 - Datasets $\leq 3.1.0$
 - Accelerate $\geq 0.26.0$

I.5 Compute Resources

We report the compute resources used for training our models in Table 13. All training was conducted on internal servers equipped with NVIDIA H100 GPUs. We estimate GPU-hours by multiplying wall-clock training time by the number of GPUs used. No additional compute was used beyond the reported experiments; we did not perform parameter grid search, large-scale hyperparameter tuning, or exploratory runs that were excluded from the paper.

Table 13: Training compute resources for zip2zip experiments.

Model	GPUs	Time	GPU Type	GPU-Hours
Phi-3-Medium (14B)	4	15h 46m	NVIDIA H100 80GB	63.0
Phi-3.5-Mini (4B)	2	7h 0m	NVIDIA H100 80GB	14.0

I.6 Evaluation

All evaluations complete within 1 hour on a single A100 GPU, demonstrating the runtime efficiency of zip2zip.

I.7 Loss Ratio

J Data Mixture

To support effective fine-tuning, we construct a curated dataset with balanced representation across diverse domains, including code, mathematics, dialogue, general web content, and multilingual text. The final dataset contains approximately 1 billion compressed tokens.

Table 14 summarizes the constituent datasets and their respective proportions. A visualization of the dataset composition and sequence length characteristics is shown in Figure 9.

The multilingual subset in fineweb-2 includes the following languages: Mandarin Chinese (cmn_Hani), German (deu_Latn), Japanese (jpn_Jpan), Spanish (spa_Latn), French (fra_Latn), Italian (ita_Latn), Portuguese (por_Latn), Dutch (nld_Latn), and Arabic (arb_Arab).

K Token Stream Visualization

Dataset	Domain	Proportion (%)
HuggingFaceFW/fineweb-edu[Lozhkov et al., 2024a]	Web / Knowledge	20%
devngho/the-stack-llm-annotations-v2[Lozhkov et al., 2024b]	Code	25%
AI-MO/NuminaMath-1.5[LI et al., 2024]	Math	20%
HuggingFaceH4/ultrachat_200k[Ding et al., 2023]	Chat / Dialogue	20%
HuggingFaceFW/fineweb-2[Penedo et al., 2024]	Multilingual	15%

Table 14: Training data composition across domains.

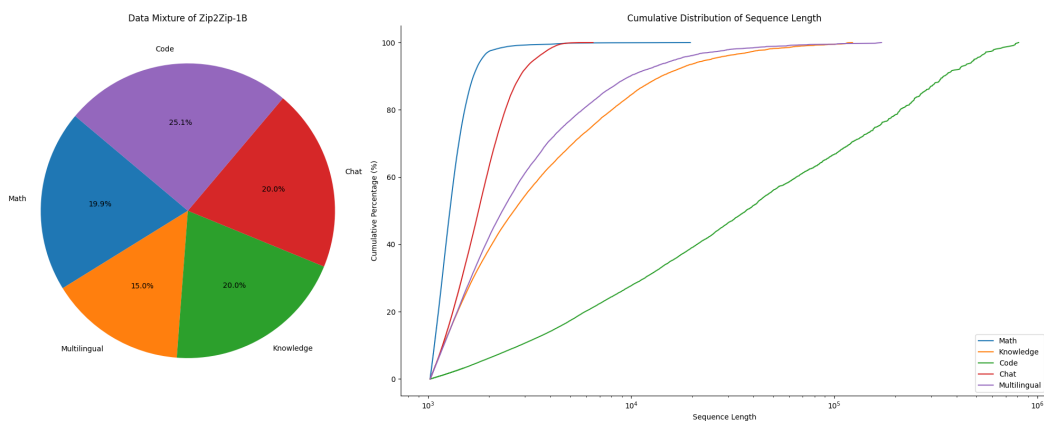


Figure 9: Left: Proportional breakdown of the fine-tuning dataset across five domains. Right: Cumulative distribution of input sequence lengths per domain (log scale). Code and multilingual data exhibit longer tail distributions, indicating greater variability in sequence lengths.

```

class GPAttention(nn.Module):
    def __init__(self, config, is_cross_attention=False, layer_idx=None):
        super().__init__()
        self.config = config
        self.max_positions = config.max_position_embeddings
        self.register_buffer(
            "bias",
            torch.tril(torch.ones((max_positions, max_positions), dtype=torch.bool)).view(
                -1, max_positions, max_positions)
        ), persistent=False
        self.register_buffer("masked_bias", torch.tensor(-1e4), persistent=False)

        self.embed_dim = config.hidden_size
        self.num_heads = config.num_attention_heads
        self.head_dim = self.embed_dim // self.num_heads
        self.split_size = self.embed_dim

        self.scale_attn_weights = config.scale_attn_weights
        self.is_cross_attention = is_cross_attention

        # Layer-wise attention scaling, reordering, and upcasting
        self.layer_idx = layer_idx
        self.reorder_and_upcast_attn = config.reorder_and_upcast_attn

        if self.is_cross_attention:
            self.q_attn = Conv1D(2 * self.embed_dim, self.embed_dim)
        else:
            self.q_attn = Conv1D(3 * self.embed_dim, self.embed_dim)
        self.c_proj = Conv1D(self.embed_dim, self.embed_dim)

        self.attn_dropout = nn.Dropout(config.attn_dropout)
        self.resid_dropout = nn.Dropout(config.resid_dropout)
        self.is_causal = True

        self.pruned_heads = set()

```

(a) Default Tokenization of some Python code.

```

class GPAttention(nn.Module):
    def __init__(self, config, is_cross_attention=False, layer_idx=None):
        super().__init__()
        self.config = config
        self.max_positions = config.max_position_embeddings
        self.register_buffer(
            "bias",
            torch.tril(torch.ones((max_positions, max_positions), dtype=torch.bool)).view(
                -1, max_positions, max_positions)
        ), persistent=False
        self.register_buffer("masked_bias", torch.tensor(-1e4), persistent=False)

        self.embed_dim = config.hidden_size
        self.num_heads = config.num_attention_heads
        self.head_dim = self.embed_dim // self.num_heads
        self.split_size = self.embed_dim

        self.scale_attn_weights = config.scale_attn_weights
        self.is_cross_attention = is_cross_attention

        # Layer-wise attention scaling, reordering, and upcasting
        self.scale_attn_by_inverse_layer_idx = config.scale_attn_by_inverse_layer_idx
        self.layer_idx = layer_idx
        self.reorder_and_upcast_attn = config.reorder_and_upcast_attn

        if self.is_cross_attention:
            self.q_attn = Conv1D(2 * self.embed_dim, self.embed_dim)
        else:
            self.q_attn = Conv1D(3 * self.embed_dim, self.embed_dim)
        self.c_proj = Conv1D(self.embed_dim, self.embed_dim)

        self.attn_dropout = nn.Dropout(config.attn_dropout)
        self.resid_dropout = nn.Dropout(config.resid_dropout)
        self.is_causal = True

        self.pruned_heads = set()

```

(b) The same code with adaptive tokenization.

```

Transcription
Main article: Transcription (genetics)
Transcription is when RNA is copied from DNA. During transcription, RNA polymerase makes a copy of a gene from the DNA to mRNA as needed. This process differs slightly in eukaryotes and prokaryotes. One notable difference is that prokaryotic RNA polymerase associates with DNA-processing enzymes during transcription so that processing can proceed during transcription. Therefore, this causes the new mRNA strand to become double stranded by producing a complementary strand known as the rRNA strand, which is the complementary strand of rRNA, which is identical in sequence to the anticodon sequence that the DNA binds to. The short-lived, unprocessed or partially processed product is termed precursor mRNA, or pre-mRNA, once completely processed, it is termed mature mRNA. [citation needed]

uracil substitution for thymine
RNA uses uracil (U) instead of thymine (T) in DNA. uracil (U) is the complementary base to adenine (A) during transcription instead of thymine (T). Thus, when using a template strand of DNA to build RNA, thymine is replaced with uracil. This substitution allows the mRNA to carry the appropriate genetic information from DNA to the ribosome for translation. Regarding the natural history, uracil can be a first then thymine, evidence suggests that RNA came before DNA in evolution. [1] The RNA World hypothesis proposes that life began with RNA molecules, because the emergence of DNA genomes and coded proteins. In DNA, the evolutionary substitution of thymine for uracil may have increased DNA stability and improved the efficiency of DNA replication. [2][3]

Eukaryotic pre-mRNA processing
Main article: Posttranscriptional modification
DNA gene is transcribed to pre-mRNA, which is then processed to form mature mRNA, and then lastly translated by a ribosome to a protein. Processing of mRNA differs greatly among eukaryotes, bacteria, and archaea. Non-eukaryotic mRNA is, in essence, mature upon transcription and requires no processing, except in rare cases. [4] Eukaryotic pre-mRNA, however, requires several processing steps before its transport to the cytoplasm and its translation by the ribosome.

```

(c) Default Tokenization of some biomedical text.

```

Transcription
Main article: Transcription (genetics)
Transcription is when RNA is copied from DNA. During transcription, RNA polymerase makes a copy of a gene from the DNA to mRNA as needed. This process differs slightly in eukaryotes and prokaryotes. One notable difference is that prokaryotic RNA polymerase associates with DNA-processing enzymes during transcription so that processing can proceed during transcription. Therefore, this causes the new mRNA strand to become double stranded by producing a complementary strand known as the rRNA strand, which is the complementary strand of rRNA, which is identical in sequence to the anticodon sequence that the DNA binds to. The short-lived, unprocessed or partially processed product is termed precursor mRNA, or pre-mRNA, once completely processed, it is termed mature mRNA. [citation needed]

uracil substitution for thymine
RNA uses uracil (U) instead of thymine (T) in DNA. uracil (U) is the complementary base to adenine (A) during transcription instead of thymine (T). Thus, when using a template strand of DNA to build RNA, thymine is replaced with uracil. This substitution allows the mRNA to carry the appropriate genetic information from DNA to the ribosome for translation. Regarding the natural history, uracil can be a first then thymine, evidence suggests that RNA came before DNA in evolution. [1] The RNA World hypothesis proposes that life began with RNA molecules, because the emergence of DNA genomes and coded proteins. In DNA, the evolutionary substitution of thymine for uracil may have increased DNA stability and improved the efficiency of DNA replication. [2][3]

Eukaryotic pre-mRNA processing
Main article: Posttranscriptional modification
DNA gene is transcribed to pre-mRNA, which is then processed to form mature mRNA, and then lastly translated by a ribosome to a protein. Processing of mRNA differs greatly among eukaryotes, bacteria, and archaea. Non-eukaryotic mRNA is, in essence, mature upon transcription and requires no processing, except in rare cases. [4] Eukaryotic pre-mRNA, however, requires several processing steps before its transport to the cytoplasm and its translation by the ribosome.

```

(d) The same text with adaptive tokenization.

```

L'impressionnisme est un mouvement pictural né en France dans les années 1860 en opposition à l'art académique et visant à représenter le caractère éphémère de la lumière et ses effets sur les couleurs et les formes. Le mouvement des impressionnistes se forme autour d'Édouard Manet, chef de file de l'avant-garde artistique dans les années 1860, qui ne participe cependant à aucune exposition impressionniste. Après plusieurs scandales et refus au Salon, la grande exposition annuelle d'artistes agréés par l'Académie des Beaux-Arts de jeunes artistes décide de s'associer pour organiser des expositions indépendantes. Cette idée se concrétise en 1874, dans une exposition qui réunit trente artistes dont Paul Cézanne, Eugène Boudin, Claude Monet, Berthe Morisot, Camille Pissarro, Auguste Renoir et Alfred Sisley. Le journaliste satirique Louis Leroy invente alors le terme « impressionnisme » à partir du tableau Impression, soleil levant de Monet, devenu depuis l'étendard du mouvement. Les artistes subissent d'abord des critiques acerbes de la part de la presse et du public, mais ils sont soutenus par des collectionneurs qui permettent la tenue de leurs premières expositions, notamment Gustave Gullotta.

L'impressionnisme commence à être accepté en 1880, grâce au soutien du nouveau gouvernement de Léon Gambetta et de critiques comme Félix Zola. Les œuvres font petit à petit leur entrée dans les musées, au Salon des artistes français, qui succède au Salon de l'Académie des Beaux-Arts. Quel que soit le marché de l'art, le marchand Paul Durand-Ruel joue un rôle crucial dans le soutien et la diffusion de l'impressionnisme, qui s'exporte aux États-Unis à partir de 1886, grâce à la peintre Mary Cassatt. Le mouvement y obtient un grand succès, qui participe à la consécration de Monet et au développement d'écoles impressionnistes hors de France au cours des années 1890. Cette décennie voit la mort de Morisot, Caillebotte et Sisley et la dispersion du groupe, tandis que se développent de nouvelles avant-gardes auxuelles adhèrent certains impressionnistes, comme Cézanne et Pissarro.

Les artistes impressionnistes créent une nouvelle esthétique, rompant à l'art académique. Leur style n'est pas pour la première fois dans les toiles peintes par Monet et Renoir à l'huile sur toile à Gouville, en 1869. Ils font primer la couleur sur le dessin, utilisent des compositions inhabituelles et une touche rapide, et composent généralement en plein air sur le motif. Tournez vers des sujets modernes, ils représentent principalement des paysages, des scènes de la vie intime et les loisirs de leur époque.

Les impressionnistes dans les collections muséales
L'impressionnisme est un mouvement largement porté par des artistes français. Il est logique de trouver de nombreuses œuvres dans des musées situés en France. Toutefois, la plupart des grandes collections d'art moderne à travers le monde s'efforcent également de présenter au moins quelques œuvres de toiles impressionnistes.

```

(e) Default Tokenization of text in French.

```

L'impressionnisme est un mouvement pictural né en France dans les années 1860 en opposition à l'art académique et visant à représenter le caractère éphémère de la lumière et ses effets sur les couleurs et les formes. Le mouvement des impressionnistes se forme autour d'Édouard Manet, chef de file de l'avant-garde artistique dans les années 1860, qui ne participe cependant à aucune exposition impressionniste. Après plusieurs scandales et refus au Salon, la grande exposition annuelle d'artistes agréés par l'Académie des Beaux-Arts de jeunes artistes décide de s'associer pour organiser des expositions indépendantes. Cette idée se concrétise en 1874, dans une exposition qui réunit trente artistes dont Paul Cézanne, Eugène Boudin, Claude Monet, Berthe Morisot, Camille Pissarro, Auguste Renoir et Alfred Sisley. Le journaliste satirique Louis Leroy invente alors le terme « impressionnisme » à partir du tableau Impression, soleil levant de Monet, devenu depuis l'étendard du mouvement. Les artistes subissent d'abord des critiques acerbes de la part de la presse et du public, mais ils sont soutenus par des collectionneurs qui permettent la tenue de leurs premières expositions, notamment Gustave Gullotta.

L'impressionnisme commence à être accepté en 1880, grâce au soutien du nouveau gouvernement de Léon Gambetta et de critiques comme Félix Zola. Les œuvres font petit à petit leur entrée dans les musées, au Salon des artistes français, qui succède au Salon de l'Académie des Beaux-Arts. Quel que soit le marché de l'art, le marchand Paul Durand-Ruel joue un rôle crucial dans le soutien et la diffusion de l'impressionnisme, qui s'exporte aux États-Unis à partir de 1886, grâce à la peintre Mary Cassatt. Le mouvement y obtient un grand succès, qui participe à la consécration de Monet et au développement d'écoles impressionnistes hors de France au cours des années 1890. Cette décennie voit la mort de Morisot, Caillebotte et Sisley et la dispersion du groupe, tandis que se développent de nouvelles avant-gardes auxuelles adhèrent certains impressionnistes, comme Cézanne et Pissarro.

Les artistes impressionnistes créent une nouvelle esthétique, rompant à l'art académique. Leur style n'est pas pour la première fois dans les toiles peintes par Monet et Renoir à l'huile sur toile à Gouville, en 1869. Ils font primer la couleur sur le dessin, utilisent des compositions inhabituelles et une touche rapide, et composent généralement en plein air sur le motif. Tournez vers des sujets modernes, ils représentent principalement des paysages, des scènes de la vie intime et les loisirs de leur époque.

Les impressionnistes dans les collections muséales
L'impressionnisme est un mouvement largement porté par des artistes français. Il est logique de trouver de nombreuses œuvres dans des musées situés en France. Toutefois, la plupart des grandes collections d'art moderne à travers le monde s'efforcent également de présenter au moins quelques œuvres de toiles impressionnistes.

```

(f) The same text with adaptive tokenization.

Figure 10: Examples comparing default and adaptive tokenization. Dotted-line frames highlight where the differences are most noticeable.